

The Al(Nb, Ta)Ti₋₂ substitution in titanite: the emergence of a new species?

P. Černý, M. Novák, and R. Chapman

Department of Geological Sciences, University of Manitoba, Winnipeg, Manitoba,
Canada

With 6 Figures

Received September 17, 1992;
accepted January 31, 1994

Summary

The highest (Nb, Ta) content ever encountered in titanite is reported from the Maršíkov II pegmatite in northern Moravia, Czech Republic. This dike is a member of a pegmatite swarm of the beryl-columbite subtype, metamorphosed under conditions of the amphibolite facies. The pegmatite carries, i.e., rare tantalum rutile intergrown with titanite, titanite, titanite, titanite, fersmite and microcline. Fissures generated in the Nb, Ta oxide minerals during deformation are filled with titanite, formed by reaction of the oxide minerals with metamorphic pore fluids. The titanite displays limited degrees of substitutions $\text{Na}(\text{Ta} > \text{Nb})(\text{CaTi})_{-1}$, $(\text{Ta} > \text{Nb})_4\text{Ti}_{-4}\text{Si}_{-1}$ and $\text{Al}(\text{OH}, \text{F})(\text{TiO})_{-1}$, but an extensive (and occasionally the sole significant) substitution $(\text{Al} \gg \text{Fe}^{3+})(\text{Ta} > \text{Nb})\text{Ti}_{-2}$, responsible for widespread oscillatory zoning. This substitution reduces the proportion of the titanite component *sensu stricto*, $\text{CaTiSiO}_4\text{O}$, to less than 50 mole % in many analyzed spots. The extreme composition corresponds to $(\text{Ca}_{0.994}\text{Na}_{0.011})(\text{Ti}_{0.436}\text{Sn}_{0.007}\text{Al}_{0.280}\text{Fe}_{0.006}^{3+}\text{Ta}_{0.199}\text{Nb}_{0.079})\text{Si}_{0.988}\text{O}_4(\text{O}_{0.974}\text{F}_{0.026})$. However, so far this substitution fails to generate compositions that would define a new species.

Zusammenfassung

Die Al(Nb, Ta)Ti₋₂ Substitution im Titanit: Auftauchen einer neuen Mineralspecies?

Die höchsten (Nb, Ta) Gehalte, die jemals für Titanit gefunden wurden, werden für den Maršíkov II Pegmatit in Nordmähren, Tschechien, berichtet. Der Intrusivgang ist Teil eines Amphibolit-faziell überprägten Pegmatitschwarms vom Beryll-Columbit Subtypus. Der Pegmatit führt u.a. seltene tantalbetonte Rutilite verwachsen mit titanbetontem Ixiolith, titanbetontem Columbit-Tantalit, Fersmit und Mikrolith. Deformationsbedingte Frakturen in den (Nb, Ta) Oxiden sind mit Titanit, als Folge der Reaktion der metamorphen Porenlösungen mit den Oxidmineralen, verkittet. Titanit zeigt begrenzte

Substitutionen $\text{Na}(\text{Ta} > \text{Nb})(\text{CaTi})_{-1}$, $(\text{Ta} > \text{Nb})_4 \square \text{Ti}_{-4} \text{Si}_{-1}$ and $\text{Al}(\text{OH}, \text{F})(\text{TiO})_{-1}$, aber extensive (und gelegentlich einzig bedeutsame) Substitution $(\text{Al} \gg \text{Fe}^{3+})(\text{Ta} > \text{Nb})\text{Ti}_{-2}$, die eine weitverbreitete, oszillierende Zonierung hervorruft. Diese Substitution verringert den Anteil der Titanit-Komponente *sensu stricto*, $\text{CaTiSiO}_4\text{O}$, auf weniger als 50 Mol% in vielen Analysen. Die Extremzusammensetzung entspricht $(\text{Ca}_{0.994}\text{Na}_{0.11})(\text{Ti}_{0.436}\text{Sn}_{0.007}\text{Al}_{0.280}\text{Fe}^{3+}_{0.006}\text{Ta}_{0.199}\text{Nb}_{0.079})\text{Si}_{0.988}\text{O}_4(\text{O}_{0.974}\text{F}_{0.026})$. Das Ausmaß dieser Substitution ist unzureichend, um eine neue Mineralspecies zu definieren.

Introduction

Ever since the landmark paper by *Sahama* (1946), titanite has been known to incorporate minor to subordinate Nb and/or Ta in its structure. With progress of time, igneous geochemists recognized the potential of accessory titanite to incorporate Nb and Ta during protomagmatic crystallization, preventing these elements from accumulating in residual melts and fluids (*Tauson*, 1963, 1967). However, titanite with substantial content of Nb and Ta is rather rare. The first reports of such a titanite were published by *Semenov* (1959) and *Clark* (1974). Additional finds of Nb, Ta-rich titanite were described relatively recently (*Paul et al.*, 1981; *Groat et al.*, 1985; *Bernau and Franz*, 1987).

Stoichiometry of the Nb, Ta-rich titanite samples indicates that several substitution mechanisms may cooperate in accommodating $(\text{Nb}, \text{Ta})^{5+}$ in the Ti^{4+} sites: (i) $(\text{Al} > \text{Fe}^{3+})(\text{Nb}, \text{Ta})\text{Ti}_{-2}$, (ii) $(\text{Nb}, \text{Ta})(\text{Al}, \text{Fe}^{3+})(\text{TiSi})_{-1}$, (iii) $\text{Na}(\text{Nb}, \text{Ta})(\text{CaTi})_{-1}$. All three substitutions have the stoichiometric (although not necessarily structural) potential to generate end-member compositions, i.e. (i) $\text{Ca}(\text{Al}, \text{Fe}^{3+})_{0.5}(\text{Nb}, \text{Ta})_{0.5}\text{SiO}_4\text{O}$, (ii) $\text{Ca}(\text{Nb}, \text{Ta})(\text{Al}, \text{Fe}^{3+})\text{O}_4\text{O}$, (iii) $\text{Na}(\text{Nb}, \text{Ta})\text{SiO}_4\text{O}$. So far, none of the Nb, Ta-rich samples approached a composition that could establish a new species, in part because the above substitutions tend to operate in mutual combinations, and also in conjunction with other, more or less widespread substitutions: (iv) $(\text{Al}, \text{Fe}^{3+})(\text{OH}, \text{F})(\text{TiO})_{-1}$, (v) SnTi_{-1} , (vi) $(\text{Y}, \text{REE})(\text{Al}, \text{Fe}^{3+})(\text{CaTi})_{-1}$, (vii) $\text{Na}(\text{OH}, \text{F})(\text{CaO})_{-1}$, (viii) $(\text{NaP})(\text{CaSi})_{-1}$.

Here we report on a new occurrence of titanite which is unique in its origin and content of Nb and Ta. The $(\text{Al} \gg \text{Fe}^{3+})(\text{Ta} > \text{Nb})\text{Ti}_{-2}$ substitution reduces the proportion of titanite *sensu stricto* in this mineral to less than 50 mole %.

The parent pegmatite

The Ta, Nb-rich titanite described below comes from a pegmatite in the Šumperk-Maršíkov pegmatite district, in the southern part of the pegmatite field of Hrubý Jeseník Mts. in northern Moravia, Czech Republic (Fig. 1). This dike, designated Maršíkov II, is a member of the metamorphosed pegmatite swarm outcropping on the hill Schinderhübel, some 600 m NE of the village of Maršíkov. Sillimanite-grade metamorphism and shearing produced abundant chrysoberyl in this swarm (*Hruschka*, 1824; *Franz and Morteani*, 1984; pegmatite III), and considerably modified the chemical and phase composition of Nb, Ta oxide minerals (*Černý et al.*, 1992; pegmatites I and III).

The pegmatite II is poorly exposed; we have only a very sketchy knowledge of its composition. Its internal structure is virtually unknown, except for the presence

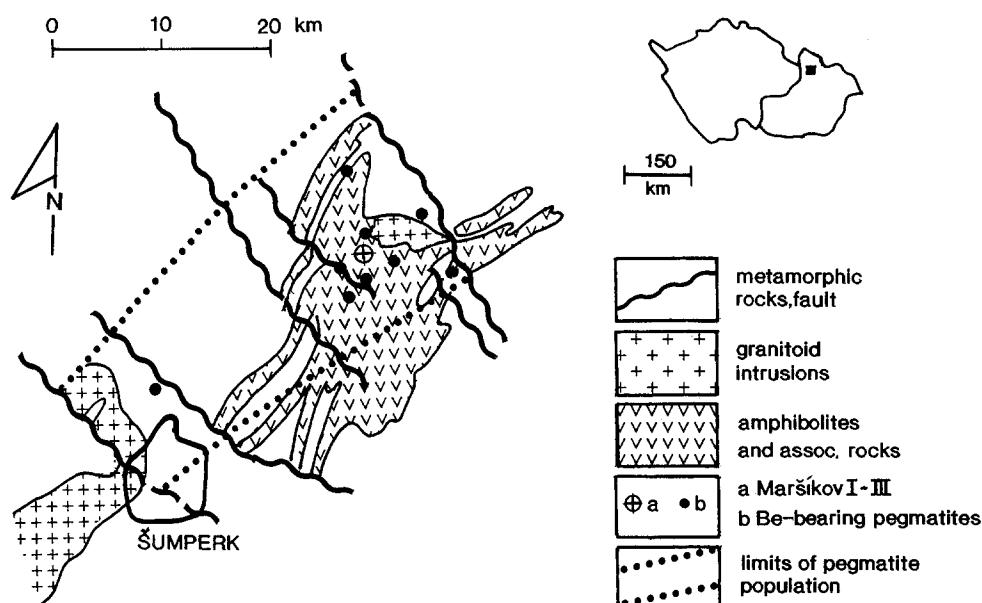


Fig. 1. Location of the Maršíkov pegmatites in northern Moravia, Czech Republic

of a quartz core. Weathered rubble suggests that this pegmatite may be close to the $Ab + Qtz + Ms$ composition of dikes I and III, with minor, if any, Kfs. Accessory garnet ($Sps_{71.5-61.2}Alm_{33.4-26.7}Prp_{4.4-1.5}Grs_{1.1-0.4}$), zircon, chrysoberyl, sillimanite, hornblende and rare magnetite are dispersed through some samples, the last two being suggestive of contamination of the pegmatite by reaction with the enclosing hornblende-biotite gneiss. Late epidote and chlorite are locally observed. Minerals of Nb and Ta are represented by scarce grains of tantalian rutile, intergrown with titanian ixiolite, titanian columbite-tantalite, fersmite and microlite and penetrated by the Ta, Nb-rich titanite.

Experimental methods

Electron microprobe analyses were carried out in the wavelength dispersion mode on a Cameca Camebax SX50 instrument, with beam diameter of 1–2 μm and an accelerating potential of 15 kV. For titanite, a sample current of 20 nA measured on Faraday cup and a counting time of 20s were used for Na, Ca, Fe, Ti and Si, 20 nA and 50s for F, U and 40 nA plus 50s for Mn, Al, Sn, Ta and Nb. Sodium was analyzed first to minimize its volatilization. The following standards (natural by mineral names, synthetic by formulas) were used: microlite (NaK α , FK α), titanite (TiK α , SiK α), $FeNb_2O_6$ (FeK α), $CaNb_2O_6$ (CaK α), UO_2 (UM β), pyrope (AlK α), manganotantalite (TaL α), $MnNb_2O_6$ (NbL α , MnL α) and SnO_2 (SnL α). The standards were selected, crossanalyzed, and their compositions refined at our laboratory since 1984. Conditions and standards applied to the analysis of the oxide minerals of Nb and Ta were those quoted by Černý et al. (1992). Each grain was analyzed at 3 to 8 spots, depending on its size. Data were reduced using the PAP routine of Pouchou and Pichoir (1985).

Formulas of rutile and columbite-tantalite are calculated on the basis of 4 and 24 oxygens, respectively, per their unit-cell contents. The cation content of titanian ixiolite is calculated for 24 oxygens of the ordered columbite cell (see, e.g., Černý and Ercit 1989, for definition), to facilitate direct comparison with titanian columbite-tantalite. In cases of

cations excessive over the available structural sites, adjustment for Fe^{3+} is based on both cation and oxygen normalization. Cation contents of microlite are based on $\Sigma(\text{Nb}, \text{Ta}, \text{Ti}, \text{Sn}) = 2$ p.f.u. (per formula unit), whereas those of fersmite are calculated for $\Sigma \text{ cat.} = 3$ p.f.u., with OH derived from stoichiometry. Formulas of titanite are based on $\Sigma \text{ cat.} = 3$ p.f.u., assuming all Fe in trivalent state and calculating (O, OH) in the O(1) site by stoichiometry and charge balance (except the Na-enriched compositions normalized to 5 anions, as discussed under “Titanite”).

The Philips PW 1710 instrument was used to confirm the identity of the examined phases by X-ray powder diffraction.

Oxide minerals of Ti, Nb and Ta

Tantalian rutile comprises aggregates up to 8 mm in size, fairly coarse-grained and compositionally heterogeneous, imbedded in aggregates of albite and quartz (Fig. 2A). Very low $\text{Mn}/(\text{Mn} + \text{Fe})$ (at.) is observed (Fig. 3A), as characteristic of this mineral in virtually all of its occurrences (e.g., Černý and Ercit, 1989), and a relatively low $\text{Fe}^{2+}/\text{Fe}^{3+}$ ratio (Fig. 3b). Representative chemical compositions are shown in Table 1. X-ray powder diffraction indicates a disordered structure of the monorutile type (cf., e.g., Černý and Ercit, 1989).

Phases related to the columbite-structure type are present in two varieties, provisionally termed titanian ixiolite and titanian columbite-tantalite. This tentative identification is based on their contrasting chemistry, and on X-ray powder diffraction patterns corresponding to the disordered columbite structure (as defined, e.g., in Černý and Ercit, 1989). Heating experiments that would unambiguously identify the first of the above phases as ixiolite or extremely titanian columbite-tantalite (cf. Černý and Ercit, 1989) could not be performed because of scarcity and microscopic size of the mineral.

Titanian ixiolite forms irregular grains or stringers, locally with euhedral ghost surfaces revealed by oscillatory variations in Nb and Ta on BSE images. The ixiolite

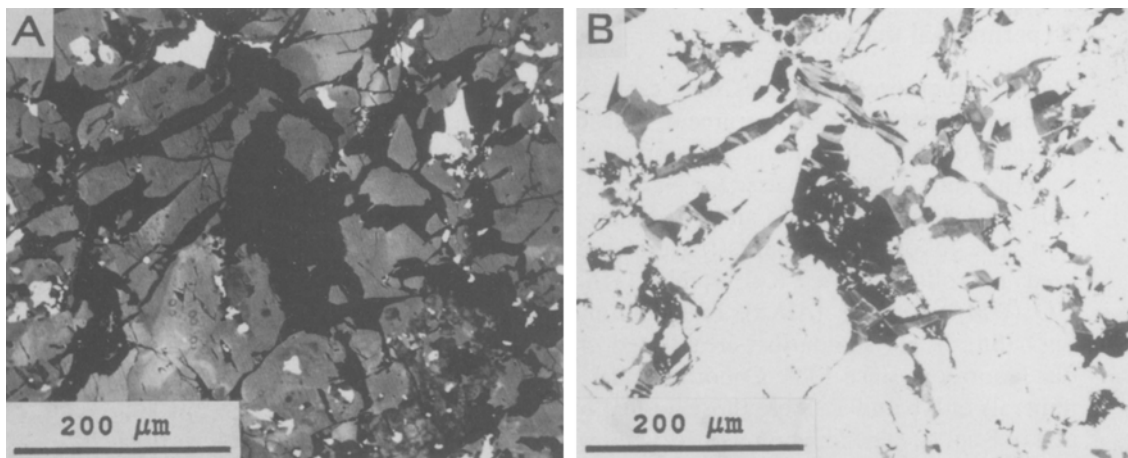


Fig. 2. **A** Tantalian rutile (dark) with grains of titanian columbite-tantalite and titanian ixiolite (white). **B** Same area as in A; the Nb, Ta, Ti oxide minerals (white) show angular fissures filled with titanite (mottled grey; black plucking hole near centre). Backscattered electron images at different offsets

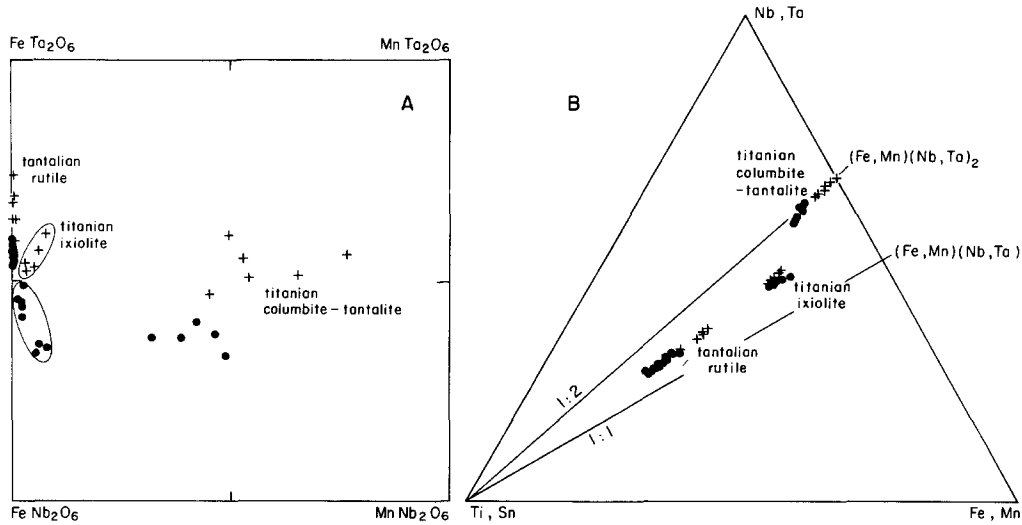


Fig. 3. **A** Compositions of tantalian rutile, titanian ixiolite and titanian columbite-tantalite in the columbite quadrilateral (molecular proportions). The fields of titanian ixiolite are identified by outlines. Compositions analyzed in two separate mineral aggregates (dots and crosses) are distinguished by an overall shift in the Ta/Nb ratio. **B** The same minerals in a ternary (Ti, Sn)–(Nb, Ta)–(Fe, Mn) diagram (same symbols as in A); high proportion of Fe³⁺ in tantalian rutile and titanian ixiolite is indicated by their positions intermediate between the 1 : 2 and 1 : 1 lines

is Mn-poor but remarkably Ti- and Fe³⁺-rich, close to the Fe-sideline of the columbite quadrilateral (Fig. 3A, B). In contrast, the columbite-tantalite composes small anhedral grains, largely less than 50 μm in size (Fig. 2A). Their atomic ratios Mn/(Mn + Fe) and Ta/(Ta + Nb) are highly variable, covering the central parts of the quadrilateral; however, the proportions of Ti and Fe³⁺ are much lower relative to those of the ixiolite (Fig. 3A, B). Representative chemical compositions of both minerals are shown in Table 1.

Fersmite and microlite form rare and very fine grains, in many cases close to the resolution limit of the electron beam. They are identified only by composition because X-ray diffraction was not feasible. Fersmite is rich in Ti and hydroxyl, whereas F and REE's were not detected; the Ta/(Ta + Nb) atomic ratio locally exceeds 0.50. The fersmite shows the so far unexplained but typical slight excess of the large A-site cations, compensated by deficiency in the B site (cf., e.g., Foord and Mrose, 1978; Černý et al., 1992). Microlite is enriched in Ti but relatively poor in Na and F, and it shows the typical deficiency in the A site (cf. Černý and Ercit, 1989). Representative compositions of fersmite and microlite are shown in Table 2.

Titanite

Anhedral grains of titanite fill angular fissures dispersed in the tantalian rutile, in aggregates up to 40 × 150 μm in size (Fig. 2B). Oscillatory zoning is typical of most of its grains (Fig. 4). The mineral was identified by a few X-ray powder diffractions only in a bulk sample consisting mainly of the host tantalian rutile with minor columbite-type phases.

Table 1. Chemical composition of titanian columbite-tantalite, titanian ixiolite and tantalian rutile from Maršíkov II

	Columbite-tantalite		Titanian ixiolite		Tantalian rutile	
	5	12	50	19	15a	15b
WO ₃	0.07	0.00	0.19	0.00	0.07	0.00
Nb ₂ O ₅	39.28	26.71	28.05	18.85	16.93	9.83
Ta ₂ O ₅	34.01	54.44	32.97	48.23	31.92	46.78
SnO ₂	0.44	0.04	0.81	0.12	0.53	0.14
TiO ₂	7.68	1.84	15.13	11.81	34.51	26.49
ZrO ₂	0.00	0.00	0.03	0.18	0.00	0.00
UO ₂	0.13	0.11	0.11	0.15	0.07	0.07
Sc ₂ O ₃	0.54	0.00	0.15	0.04	0.09	0.00
Sb ₂ O ₃	0.02	0.01	0.02	0.00	0.04	0.02
Fe ₂ O ₃ *	5.66	1.83	14.87	17.60	9.72	11.13
FeO	10.45	5.94	4.90	3.01	5.18	4.94
MnO	1.47	8.31	0.53	1.35	0.02	0.16
MgO	0.67	0.49	0.43	0.34	0.07	0.07
CaO	0.16	0.01	0.02	0.01	0.02	0.01
	100.58	99.73	98.21	101.69	99.17	99.64
W	0.004	0.000	0.012	0.000	0.001	0.000
Nb	4.358	3.415	3.045	2.124	0.281	0.178
Ta	2.270	4.186	2.153	3.269	0.319	0.509
Sn	0.043	0.005	0.078	0.012	0.008	0.002
Ti	1.417	0.391	2.732	2.213	0.954	0.798
Zr	0.000	0.000	0.004	0.022	0.000	0.000
U	0.007	0.007	0.006	0.008	0.001	0.001
Sc	0.115	0.000	0.031	0.009	0.003	0.000
Sb	0.002	0.001	0.002	0.000	0.001	0.000
Fe ³⁺	1.045	0.390	2.687	3.302	0.269	0.335
Fe ²⁺	2.144	1.405	0.984	0.627	0.159	0.166
Mn	0.306	1.990	0.108	0.285	0.001	0.005
Mg	0.245	0.207	0.154	0.126	0.004	0.004
Ca	0.042	0.003	0.005	0.003	0.001	0.000
	11.998	12.000	12.001	12.000	2.002	1.998
Ta/(Ta + Nb) at.	0.34	0.55	0.30	0.61	0.53	0.74
Mn/(Mn + Fe) at.	0.37	0.59	0.10	0.32	0.01	0.03
Fe ³⁺ /(Fe ³⁺ + Fe ²⁺) at.	0.24	0.22	0.73	0.84	0.63	0.67

* Fe₂O₃ calculated by charge-balancing to Σ cat. = 12 and 24 oxygens per ordered unit cell of columbite-tantalite, and to Σ cat. = 2 and 4 oxygens per unit cell of rutile, from Σ Fe determined as FeO. As and Bi not detected in any of the analyzed grains

Chemical composition of the titanite, examined by a total of 83 electron microprobe analyses, shows variable but persistently high contents of Ta and Nb, coupled mainly with increased Al (Table 3). The contents of Na and F are in most cases minor but locally do attain noticeably elevated values. In a few analyzed spots, U and Sn increase above their low average concentrations to 1.33 wt.% UO₂ and 1.79 SnO₂. However, even these contents are negligible atomically (0.011 and 0.027 atoms p.f.u., respectively).

Plots of (Al, Fe³⁺) vs (Nb, Ta) and Na vs (Nb, Ta) (Fig. 5A, B) show erratic trends that conform to the respective stoichiometries of substitutions (i), (ii) and (iii) only in limited segments. Figure 5A shows extensive scatter around the compositions conforming to the substitutions (i) and/or (ii), and Fig. 5B suggests that a signifi-

Table 2. Chemical composition of fersmite and microlite from Maršikov II

	Fersmite				Microlite	
	52	53	5n1	5n6	301	57
Nb ₂ O ₅	46.77	38.24	35.76	25.83	16.51	12.18
Ta ₂ O ₅	30.18	33.27	31.40	47.32	47.48	49.93
TiO ₂	4.42	9.34	12.40	7.41	6.60	7.26
UO ₂	0.05	0.03	0.58	1.00	0.00	0.06
SnO ₂	0.18	0.38	0.08	0.08	1.11	1.17
Y ₂ O ₃	0.01	0.04	0.09	0.07	0.00	0.00
CaO	15.28	15.87	15.72	13.85	18.96	19.75
MnO	0.17	0.02	0.02	0.09	0.19	0.26
FeO	0.38	0.49	0.56	0.36	0.56	0.76
BaO	0.00	0.03	0.06	0.06	0.06	0.09
Na ₂ O	0.00	0.00	0.00	0.00	0.45	0.12
K ₂ O	0.00	0.00	0.02	0.02	0.00	0.00
F	0.00	0.00	0.00	0.00	1.10	0.93
-O=F	0.00	0.00	0.00	0.00	0.46	0.39
	97.44	97.71	96.69	96.09	92.56	92.12
Nb	1.279	1.017	0.940	0.767	0.579	0.440
Ta	0.496	0.532	0.496	0.845	1.002	1.086
Ti	0.201	0.413	0.542	0.366	0.385	0.437
Sn ⁴⁺	0.004	0.009	0.002	0.002	0.034	0.037
	1.980	1.971	1.980	1.980	2.000	2.000
Ca	0.990	1.001	0.979	0.975	1.576	1.692
Ba	0.000	0.001	0.001	0.002	0.002	0.003
Fe ²⁺	0.019	0.024	0.027	0.020	0.036	0.051
Mn	0.009	0.001	0.001	0.005	0.012	0.018
Na	0.000	0.000	0.000	0.000	0.068	0.019
K	0.000	0.000	0.001	0.002	0.000	0.000
U ⁴⁺	0.001	0.000	0.008	0.015	0.000	0.001
Y	0.000	0.001	0.003	0.002	0.000	0.000
	1.019	1.028	1.020	1.021	1.694	1.784
O	5.738	5.496	5.412	5.602	6.000	6.075
F	0.000	0.000	0.000	0.000	0.270	0.235
OH	0.262	0.504	0.588	0.398	0.630	0.690

Fersmite normalized to Σ cat. = 3 p.f.u., and microlite to $\Sigma(\text{Nb, Ta, Ti, Sn}^{4+}) = 2$ p.f.u.; OH calculated from charge balance and stoichiometry. W, Sb, As, Bi, Sc, Sr and Mg were not detected in any of the analyzed grains

cant degree of substitution (iii) is accomodated only when 0.25 (Nb, Ta) p.f.u. were substituted by other mechanisms. All this indicates that several substitutions operate in most compositions in a complex and possibly interdependent manner. Nevertheless, consideration of the above trends and of the distribution of data points in Fig. 6A indicate that three types of titanite compositions can be distinguished, more or less randomly distributed over the examined Nb, Ta oxide-mineral aggregates but with distinct local accumulations: Al(Nb, Ta)-rich, Na(Nb, Ta)-enriched and Al(F, OH)-enriched.

In the first compositional type, (Ta, Nb) is well balanced by Al (Fig. 5A, B). The substitution (i), $(\text{Al} \gg \text{Fe}^{3+})(\text{Ta} > \text{Nb})\text{Ti}_{2-}$, is clearly predominant in 13 analyzed spots, up to the virtual exclusion of any other mechanism. The contents of Na, F and calculated OH are negligible in this variety, and they do not account for

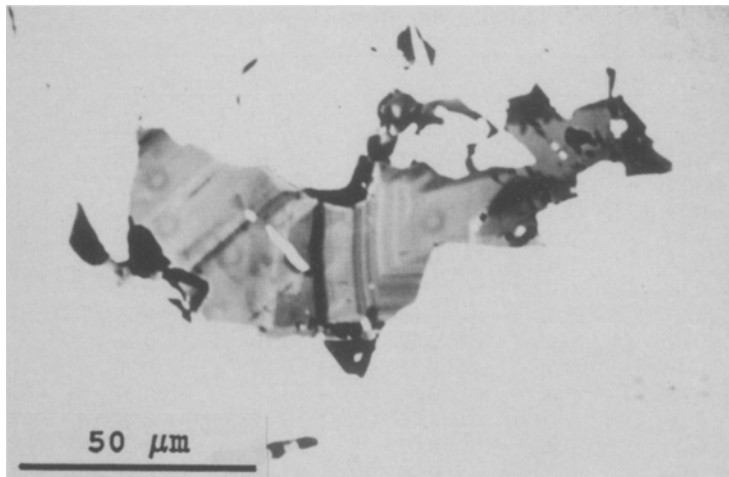


Fig. 4. Anhedral grains of titanite filling a fissure in tantalian rutile, with oscillatory compositional zoning. Backscattered electron image

incorporation of more than 0.02 (Ta, Nb) or 0.04 (Al, Fe³⁺) p.f.u., respectively, into the Ti site. In contrast, (Al ≫ Fe³⁺) balances 95–100% of (Ta > Nb); the couple substitutes for up to 0.56 Ti p.f.u. (cf. 314b and 33cl in Table 3). The extreme composition yields the formula (Ca_{0.994}Na_{0.011})(Ti_{0.436}Sn_{0.007}Al_{0.280}Fe_{0.006}³⁺·Ta_{0.199}Nb_{0.079})Si_{0.988}O₄(O_{0.974}F_{0.026}).

These titanite compositions generate balanced site populations and charge distributions when normalized to 3 cations. However, the Na-rich compositions of the second category, with (Ta, Nb) much in excess of (Al, Fe³⁺) (Fig. 6A), do not respond to such a treatment. They show excessive sums of cation charges which require divalent anions above the structurally feasible maximum of 5 by 0.039–0.073 p.f.u. The only realistic formulas that fit the crystal-chemical constraints of titanite are produced by recalculation based on 5 anions p.f.u. Good charge balance and site occupancies are achieved this way, but for the price of generating cation vacancies, so far unheard of in titanite. On this basis, the entry of (Ta, Nb) into the Na-rich titanite can be explained by a combination of three substitution mechanisms: 30 to 35% of (Ta, Nb) is balanced by (Al, Fe³⁺) in the Ti site via substitution (i), 25 to 28% of (Ta, Nb) is balanced by Na in the substitution (iii), Na(Ta, Nb)(CaTi)₋₁, and the remaining 36–39% of (Ta, Nb) is involved in a previously unsuspected substitution (ix) (Ta, Nb)₄□Ti₋₄Si₋₁. This substitution is confirmed by the deficit in Si, which is significantly greater here (0.027–0.050 p.f.u.) than in any other type of the examined titanite compositions, and by the near-ideal occupancies of the Ca site (Ca, Na, Mn, U) and Ti site (Ti, Sn, Ta, Nb, Al, Fe³⁺). Experimental difficulties were cited as the cause of slight deficiencies in Si (<0.03 p.f.u.) in titanite (Franz and Spear, 1985; Oberti et al., 1991). However, the above facts indicate that in the present case the tetrahedral vacancies are real. Compositions 33bl and 348d in Table 3 are representative in this and other respects of the 9 Na-rich compositions examined here in detail.

The third significant but least widespread type of composition is enriched in (F, OH), and shows (Al, Fe³⁺) much in excess of (Ta, Nb) (Fig. 6A). Substitution (i) balances here all (Ta, Nb) by an equal number of (Al, Fe³⁺), and the

Table 3. Chemical composition of titanite from Maršikov II

	(Al ≫ Fe ³⁺) (Ta > Nb)-substituted						Na-enriched		F-enriched	
	317b	319b	111b	315b	314b	33cl	33b1	348d	538	314
Nb ₂ O ₅	3.16	2.75	3.14	4.47	4.12	4.76	7.81	9.49	5.35	4.86
Ta ₂ O ₅	21.27	21.34	21.53	18.13	20.81	19.94	19.57	18.98	17.31	10.76
TiO ₂	17.23	16.97	16.36	16.51	15.92	15.83	19.22	18.16	14.84	18.68
SiO ₂	26.92	26.78	26.99	27.24	26.84	26.95	25.90	25.18	27.48	29.21
UO ₂	0.06	0.08	0.00	0.00	0.07	0.00	0.00	0.03	0.00	0.03
SnO ₂	0.38	0.45	0.45	0.61	0.55	0.49	0.46	0.44	0.50	0.77
Al ₂ O ₃	5.92	6.02	5.99	6.67	6.65	6.47	2.23	2.07	7.70	6.62
Fe ₂ O ₃	0.15	0.26	0.23	0.21	0.22	0.23	0.73	1.07	0.15	0.16
CaO	25.07	24.95	24.96	25.59	25.32	25.30	22.73	22.06	25.66	26.88
MnO	0.03	0.00	0.02	0.01	0.01	0.01	0.00	0.00	0.01	0.00
Na ₂ O	0.21	0.23	0.25	0.09	0.19	0.15	1.20	1.28	0.16	0.09
F	0.04	0.07	0.06	0.15	0.11	0.22	0.00	0.03	0.59	0.70
-O=F	0.02	0.03	0.03	0.06	0.05	0.09	0.00	0.01	0.25	0.29
	100.42	99.87	99.95	99.62	100.76	100.26	99.85	98.78	99.50	98.47
Ca	0.987	0.987	0.988	0.997	0.992	0.994	0.912	0.899	0.994	1.009
Mn	0.001	0.000	0.001	0.000	0.000	0.000	0.000	0.000	0.000	0.000
Na	0.015	0.016	0.018	0.006	0.013	0.011	0.087	0.094	0.011	0.006
U	0.000	0.001	0.000	0.000	0.001	0.000	0.000	0.000	0.000	0.000
	1.003	1.004	1.007	1.003	1.006	1.005	0.999	0.993	1.005	1.015
Ti	0.476	0.471	0.454	0.452	0.438	0.436	0.541	0.519	0.404	0.492
Nb	0.052	0.046	0.052	0.074	0.068	0.079	0.132	0.163	0.087	0.077
Ta	0.213	0.214	0.216	0.179	0.207	0.199	0.199	0.196	0.170	0.103
Al	0.256	0.262	0.261	0.286	0.286	0.280	0.098	0.093	0.328	0.273
Fe ³⁺	0.004	0.007	0.006	0.006	0.006	0.006	0.021	0.031	0.004	0.004
Sn ⁴⁺	0.006	0.007	0.007	0.009	0.008	0.007	0.007	0.007	0.007	0.011
	1.007	1.007	0.996	1.006	1.013	1.007	0.998	1.009	1.000	0.960
Si	0.989	0.989	0.997	0.991	0.981	0.988	0.970	0.958	0.994	1.024
O	4.983	4.968	4.971	4.947	4.958	4.972	5.000	4.996	4.903	4.865
OH	0.012	0.024	0.022	0.036	0.030	0.002	-	-	0.030	0.058
F	0.005	0.008	0.007	0.017	0.013	0.026	0.000	0.004	0.067	0.078
	5.000	5.000	5.000	5.000	5.001	5.000	5.000	5.000	5.000	5.001

Atomic contents p.f.u. normalized to Σ cat. = 3, except the Na-enriched samples that are based on Σ an. = 5; the OH content was calculated from stoichiometry and charge balance

remainder of the latter is compensated by (F, OH) via the substitution (iv), (Al, Fe³⁺)(F, OH)(TiO)₋₁. The role of the mechanism (iii) involving Na is negligible in all 5 compositions of this type, represented by # 314 and 538 in Table 3.

The composition # 314 shows an isolated case of excessive Si content, associated with deficit in the Ti site and excess in the Ca site. A reversal of the Ti for Si substitution (Hollabaugh and Rosenberg, 1983) is improbable because of the considerably smaller ionic radius of Si⁴⁺. We have no explanation for this deviation from stoichiometry, which certainly goes beyond the limits of experimental error.

The other 56 compositions obtained in this study are intermediate between the three types described above, and they do not contribute any additional insights into the crystal chemistry of the Maršikov II titanite. They are, however, plotted in Fig. 5A, B and 6A, B for comparison, as they document the overall enrichment of this titanite in (Ta, Nb).

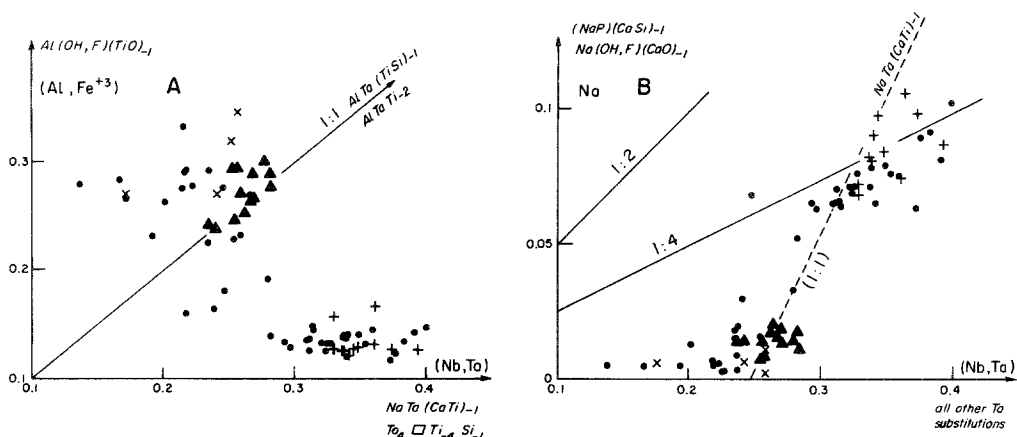


Fig. 5. **A** $(\text{Al}, \text{Fe}^{3+})$ vs (Nb, Ta) (a.p.f.u.) in titanite. Triangles—the $\text{Al}(\text{Nb}, \text{Ta})$ -rich variety; crosses—the $\text{Na}(\text{Nb}, \text{Ta})$ -enriched type; x—the $\text{Al}(\text{F}, \text{OH})$ -enriched type; dots—transitional compositions. **B** Na vs (Nb, Ta) (a.p.f.u.) in titanite; symbols as in A. Note the generally poor correlation in both diagrams; only a limited number of compositions shows a trend expected from substitution (i), $(\text{Al}, \text{Fe})(\text{Nb}, \text{Ta})\text{Ti}_{-2}$ and/or (ii), $(\text{Nb}, \text{Ta})(\text{Al}, \text{Fe}^{3+})(\text{TiSi})_{-1}$, in A, or from substitution (iii), $\text{Na}(\text{Nb}, \text{Ta})(\text{Ca}, \text{Ti})_{-1}$ in B

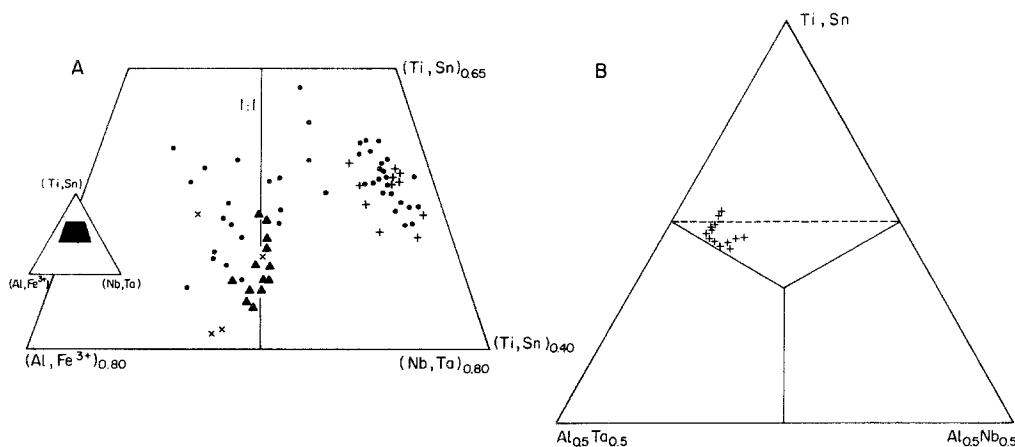


Fig. 6. **A** Titanite compositions in the ternary $(\text{Al}, \text{Fe}^{3+})$ – (Nb, Ta) – (Ti, Sn) diagram (atomic proportions); symbols as in Fig. 5A; dots mark transitional compositions. Note the position of compositions controlled by the substitution (i) along the 1 : 1 line. **B** Titanite compositions controlled by the substitution (i) (crosses in Fig. 5A, B and 6A) in the (Ti, Sn) – $(\text{Al}_{0.5}\text{Ta}_{0.5})$ – $(\text{Al}_{0.5}\text{Nb}_{0.5})$ triangle (atomic proportions). Horizontal line marks 50% of end-member titanite CaTiOSiO_4 , the others indicate subdivision of species in ternary systems, as recommended by IMA-NMMN (Nickel, 1992)

Discussion

Origin of the Nb, Ta-bearing assemblage

Sillimanite-grade metamorphism and shearing in the Maršíkov region were shown to affect pegmatite dikes I and III that developed chrysoberyl and sillimanite (Franz and Morteani, 1984) and suffered extensive adjustment of their associations of Nb,

Ta oxide minerals (at a maximum of $\sim 600^\circ\text{C}/4\text{--}6$ kbar, $P_{\text{total}} \gg P_{\text{fluid}}$; Černý et al., 1992). The assemblage of Nb, Ta oxide minerals in the Maršíkov II pegmatite also was affected, and the crystallization of titanite triggered, by metamorphism.

The primary Ta, Nb oxide mineral at Maršíkov II is the tantalian rutile. The nature of the titanian ixiolite and titanian columbite-tantalite, however, is difficult to assess. Their lower Ta/(Ta + Nb) and higher Mn/(Mn + Fe) suggest a possible exsolution relationship to the rutile phase, by analogy with the compositional characteristics of exsolved niobian rutile and titanian columbite (e.g., Černý et al., 1981). Ta-dominant rutile is usually homogeneous (Černý et al., 1981; Černý and Ercit, 1989), but it may possibly also exsolve upon deformation and metamorphism. These processes are known to promote recrystallization and equilibration in accessory minerals of Nb and Ta (e.g., Černý et al., 1989a, b). Nevertheless, the presence of two compositionally different orthorhombic phases in our tantalian rutile, and ambiguous textural relationships between all three phases do not permit any plausible interpretation at present.

Fersmite and microlite form isolated grains in apparent textural equilibrium with the present assemblage of the ferromanganoan oxide minerals of Ti, Nb and Ta. This attests to a relatively low degree of metamorphic reworking of the pegmatite II: advanced metamorphism and shearing destabilized these two minerals in dike III (Černý et al., 1992).

Whatever could have been the course of evolution of the Nb, Ta oxide minerals, it was concluded in the present form before the formation of microfractures that host the titanite. Texturally and compositionally, the titanite is a product of retrograde processes. Metamorphic pore fluids, generated mainly by dehydration reactions (Černý et al., 1992), facilitated interaction between the Nb, Ta oxide minerals and components of the silicate host rocks. These included not only the pegmatite host proper but most probably the surrounding hornblende-biotite gneiss as well; Ca is a significant component of the retrograde “alpine vein” stage in the adjacent dikes I and III (in bavenite and epidote; Černý et al., 1992), and it plays a role in the dike II as well (epidote). The highly variable chemistry of the titanite suggests low mobility of the solute reactants, heterogeneity of the fluid phase, and a lack of post-crystallizational equilibration. All of these features are compatible with the sparse volume of, and low connectivity between the titanite-hosting fissures.

Crystal chemistry of the titanite

The dominant substitution (i), $(\text{Al} \gg \text{Fe}^{3+})(\text{Ta} > \text{Nb})\text{Ti}_{-2}$, produced locally compositions in which the titanite end-member is reduced to 44 mole %. The compositions only touch the IMA-NMMN recommended boundary (Nickel, 1992) between titanite *sensu stricto* and the compositional field of a potential new species with end-member composition of $\text{CaAl}_{0.5}\text{Ta}_{0.5}\text{SiO}_4\text{O}$. Nevertheless, it may be only a matter of continuing research before compositions fitting such a species are found, possibly even in new specimens from Maršíkov.

It is noteworthy that the Maršíkov titanite exhibits a distinct dominance of Ta over Nb, despite the approximately equal proportion of these element in the precursor oxide minerals (cf. Fig. 3A). This does not seem to be a structurally controlled preference, as titanite from other localities accepts high concentrations of Nb, or Ta, or both (Clark, 1974; Paul et al., 1984; Groat et al., 1985; Bernau and Franz,

1987). The Ta > Nb composition of the Maršíkov titanite possibly reflects a greater mobility of Ta in low-temperature fluids relative to Nb, particularly in the presence of fluorine (Černý and Ercit, 1989; Černý et al., 1992).

Introduction of (Ta, Nb) into the Maršíkov titanite by the substitution (iii), $\text{Na}(\text{Ta}, \text{Nb})(\text{CaTi})_{-1}$, is persistently coupled with a vacancy-generating substitution (ix), $(\text{Ta}, \text{Nb})_4 \square \text{Ti}_{-4} \text{Si}_{-1}$. The reason could be either geochemical or structural, rooted in crystal chemistry. Increased content of Na suggests alkaline conditions of crystallization, possibly capable of generating Al-poor, slightly Si-deficient but Na, Nb, Ta-enriched titanite. Structurally, underbonding the oxygens normally coordinated with Ca^{2+} (by Na^{1+} substitution) and Si^{4+} (by vacancies) can be compensated by increased bond strength in Ti octahedra (by Nb^{5+} , Ta^{5+}). A structure refinement would be required to verify the dimensional consequences of such interplay of substitutions and bond-strength variations that are also coupled with a significant proportion of the mechanism (i). Probably both the geochemical and crystal-chemical factors contribute to the chemistry of this Na, Ta, Nb-enriched, relatively Al-poor and slightly Si-deficient titanite.

The enrichment of some of the Maršíkov titanite in (F, OH) is very restricted, noticeable only in comparison to the near-anhydrous and extremely F-poor nature of most of its compositions. Even in its scarce extreme compositions, (F, OH) does not exceed 15% of the O(1) site population.

Concluding remarks

Paul et al. (1981) suggested that (Nb, Ta)-rich titanite can be expected only in geochemically exotic environments, such as inclusions in tantalian rutile (Clark, 1974) or late, Ca-bearing stages of Ti, Nb-rich pegmatites (Paul et al., 1981). This contention is supported by the recent find in Ti, Nb, Ta-enriched pegmatitic stringers penetrating Ca-rich amphibolites (Groat et al., 1985). Peralkaline igneous assemblages constitute yet another suitable milieu (Semenov, 1959), as do calc-silicate metamorphic rocks (of unknown but possibly metasomatic origin; Bernau and Franz, 1987). The preceding description of the Maršíkov II occurrence shows that this locality ranks well with the abnormal characteristics of the others. The (Ta, Nb)-rich titanite owes its origin here to dynamothermal metamorphism of a pegmatite and its host rock, by action of pore fluids on Nb, Ta oxide minerals in retrograde conditions: a process exotic enough not to be frequently repeated elsewhere.

Acknowledgements

This study was supported by NSERC Operating and Major Installation grants to PČ, NSERC Major Equipment and Infrastructure grants to F. C. Hawthorne, and by the Dean of Science, University of Manitoba Postdoctoral Fellowship to MN. Two anonymous reviewers and P. Möller provided helpful comments.

References

- Bernau R, Franz G (1987) Crystal chemistry and genesis of Nb-, V-, and Al-rich metamorphic titanite from Egypt and Greece. *Can Mineral* 25: 695–705

- Černý P, Chapman R, Göd R, Niedermayr G, Wise MA (1989a) Exsolution intergrowth of titanian ferrocolumbite and niobian rutile from the Weinebene spodumene pegmatites, Carinthia, Austria. *Mineral Petrol* 40: 197–206
- Ercit TS (1989) Mineralogy of niobium and tantalum: crystal chemical relationships, paragenetic aspects and their economic implications. In: Möller P, Černý P, Saupé F (eds) *Lanthanides, tantalum and niobium*. Springer, SGA Spec Pub 7: 27–79
- Chapman R, Chackowsky LE, Ercit TS (1989b) A ferrotantalite-ferrotapiolite intergrowth from Spittal a.d. Drau, Carinthia, Austria. *Mineral Petrol* 41: 53–63
- Novák M, Chapman R (1992) Effects of sillimanite-grade metamorphism and shearing on Nb, Ta oxide minerals in granitic pegmatites: Maršíkov, northern Moravia, Czech Republic. *Can Mineral* 30: 699–718
- Paul BJ, Hawthorne FC, Chapman R (1981) A niobian rutile—disordered columbite intergrowth from the Huron Claim pegmatite, southeastern Manitoba. *Can Mineral* 19: 541–548
- Clark AM (1974) A tantalum-rich variety of sphene. *Mineral Mag* 39: 605–607
- Foord EE, Mrose ME (1978) Rynersonite, Ca(Ta, Nb)₂O₆, a new mineral from San Diego County, California. *Am Mineral* 63: 709–714
- Franz G, Morteani G (1984) The formation of chrysoberyl in metamorphosed pegmatites. *J Petrol* 25: 27–52
- Spear FS (1985) Aluminous titanite (sphene) from the Eclogite zone, south-central Tauern Window, Austria. *Chem Geol* 50: 33–46
- Groat LA, Carter RT, Hawthorne FC (1985) Tantalian niobian titanite from the Irgon claim, southeastern Manitoba. *Can Mineral* 23: 569–571
- Hollabaugh CL, Rosenberg PE (1983) Substitution of Ti for Si in titanite and new end-member cell dimensions for titanite. *Am Mineral* 68: 177–180
- Hruschka W (1824) Vorkommen und Kristallisation einiger mährischer Fossilien. I. Chrysoberyll. *Mitt der Mähr-Schles Gesellschaft* 52: 413–415
- Nickel EH (1992) Solid solutions in mineral nomenclature. *Can Mineral* 30: 231–234
- Oberti R, Smith DC, Rossi G, Caucia F (1991) The crystal chemistry of high-aluminum titanites. *Eur J Mineral* 3: 777–792
- Paul BJ, Černý P, Chapman R (1981) Niobian titanite from the Huron Claim pegmatite, southeastern Manitoba. *Can Mineral* 19: 549–552
- Pouchou JL, Pichoir F (1985) “PAP” (phi-rho-z) procedure for improved quantitative microanalysis. In: Armstrong JT (ed) *Microbeam analysis*. San Francisco Press, San Francisco, pp 104–106
- Sahama ThG (1946) On the chemistry of the mineral titanite. *C. R. Soc Géol Finlande* 19: 138, 88–120
- Semenov EI (1959) Mineralogy of alkaline pegmatites in the Khibiny and Lovozero tundras. *Materials on the Mineralogy of Kola Penninsula, Kirovsk*, 102–106 (in Russian)
- Tauson LV (1963) Factors in the distribution of the trace elements during the crystallization of magmas. *Phys Chem Earth* 6: 215–249
- (1967) Geochemical behavior of rare elements during crystallization and differentiation of granitic magmas. *Geokhimiya* 1967: 1310–1319 (in Russian)

Authors' addresses: P. Černý and R. Chapman, Department of Geological Sciences, University of Manitoba, Winnipeg, Manitoba, R3T 2N2, Canada; and M. Novák, Department of Mineralogy and Petrography, Moravian Museum, Zelný trh 6, 659 37 Brno, Czech Republic